First search for ultralight dark matter using a magnetically levitated particle

Amaral, D.W.P.; Uitenbroek, D.G.; Oosterkamp, T.H.; Tunnell, C.D.

First Search for Ultralight Dark Matter Using a Magnetically Levitated Particle

Dorian W. P. Amaral,[1,*] Dennis G. Uitenbroek,[2] Tjerk H. Oosterkamp,[2] and Christopher D. Tunnell[1]
[1]*Department of Physics and Astronomy, Rice University, MS-315, Houston, Texas 77005, USA*
[2]*Leiden Institute of Physics, Leiden University, P.O. Box 9504, 2300 RA Leiden, The Netherlands*

(Received 24 September 2024; revised 6 March 2025; accepted 24 April 2025; published 24 June 2025)

We perform the first search for ultralight dark matter using a magnetically levitated particle. A submillimeter permanent magnet is levitated in a superconducting trap with a measured force sensitivity of 0.2 $\mathrm{fN}/\sqrt{\mathrm{Hz}}$. We find no evidence of a signal and derive limits on dark matter coupled to the difference between baryon and lepton number, $B-L$, in the mass range $(1.10360-1.10485)\times10^{-13}\ \mathrm{eV}/c^2$. Our most stringent limit on the coupling strength is $g_{B-L}\lesssim 2.98\times10^{-21}$. We propose the POLONAISE (Probing Oscillations using Levitated Objects for Novel Accelerometry In Searches of Exotic physics) experiment, which features short-, medium-, and long-term upgrades that will give us leading sensitivity in a wide mass range, demonstrating the promise of this novel quantum sensing technology in the hunt for dark matter.

DOI: 10.1103/PhysRevLett.134.251001

Introduction—Dark matter (DM) dominates the matter content of our Universe. Yet, we know remarkably little about its fundamental nature. Except for the fact that it must interact gravitationally, important properties such as its mass, spin, and other potential interactions remain largely a mystery [1–3]. Astrophysical observations suggest that its mass can lie anywhere in the range of $10^{-19}\ \mathrm{eV}/c^2$ to a few solar masses, spanning a vast 90 orders of magnitude [4,5]. The lower end of this mass window defines the *ultralight* regime for dark matter, which has been gaining considerable attention [6,7].

In this regime, ultralight dark matter (ULDM) particles must be bosonic to reconcile the observed dark matter density. A consequence of this is that these particles exhibit wavelike behavior, leading to interference regions throughout the cosmos. Popular ultralight candidates include the QCD axion [8–10], axionlike particles as well as other scalars [11–13], and—of relevance to us—vector particles [14–16].

Ultralight vector dark matter particles are spin-1 bosons that stem from the same type of symmetry as the standard model photon. Many early Universe production mechanisms generate this type of dark matter [17–27], and the late-Universe structures that it can form have been explored via numerical simulations [28–32]. These particles can communicate with us via charges different from that of electromagnetism. In this work, we take this to be the difference between the baryon and lepton numbers of a particle, $B-L$; this leads to a well-motivated dark matter candidate [33,34] and can also help to explain the nonzero mass of neutrinos [35–37].

Many experiments have constrained the interaction strength of $B-L$ coupled dark matter, and a variety of detector technologies have been used to derive projected sensitivities. Limits have been set by fifth-force experiments, such as MICROSCOPE [38–41] and Eöt-Wash [42,43], and gravitational wave interferometers, such as LIGO/Virgo [44] and KAGRA [45], among other experiments. Projections with accelerometers have been shown to be promising [46,47], with these instruments being realized as torsion balances [46], optomechanical cavities [48,49], atomic interferometers [50], and future gravitational-wave detectors [51–54].

One detector technology undergoing a significant rate of innovation involves the levitation of macroscopic objects via magnetic Meissner levitation [55–58]. Levitated magnets are excellent force and acceleration sensors [59,60], making them ideal for detecting the minuscule signatures expected from ultralight dark matter [61–64]. The low temperatures involved in these setups provide exceptionally low thermal noise and, compared to optical and electrical levitation strategies, much larger levitated objects are possible [55]. The ability to levitate heavier objects gives us greater sensitivity to dark matter couplings proportional to mass, such as that arising from $B-L$ dark matter [64].

In this Letter, we perform the first search for ultralight dark matter using a magnetically levitated mass and propose the POLONAISE (Probing Oscillations using Levitated Objects for Novel Accelerometry In Searches

*Contact author: dorian.amaral@rice.edu

of Exotic physics) experiment. We analyze data from the setup initially described in Ref. [59] for tests of small-scale gravity, employing a sub-millimeter-sized magnetically levitated particle. Using a likelihood-led treatment to perform our inferencing, we account for the inherent stochasticity in the ULDM field. We motivate short-, medium-, and long-term upgrades to propose POLONAISE, which will allow us to achieve leading sensitivity to ULDM and highlight the advancements in quantum metrology necessary for a world-leading DM experiment.

Ultralight vector dark matter—Ultralight vector dark matter consists of spin-1 bosons with masses $m_{\rm DM}$ between 10^{-19} eV/c^2 to 2 eV/c^2 [13]. To compose all of the local dark matter density, $\rho_{\rm DM} \approx 0.4\ {\rm GeV}/c^2\,{\rm cm}^{-3}$ [65,66], their small mass results in a macroscopic number of particles within a de Broglie volume, $\lambda_{\rm dB}^3$. Assuming virialization and taking the local circular velocity to be $v_0 \approx 220\ {\rm km\,s}^{-1}$ [67], we have a total of $N_{\rm dB} \sim (\rho_{\rm DM}/m_{\rm DM})(h/m_{\rm DM}v_0)^3 \sim 10^{58}$ particles for a DM mass of $10^{-13}\ {\rm eV}/c^2$. Consequently, DM particles within the halo behave more as classical waves than particles.

Within a de Broglie volume, these DM waves oscillate coherently at their Compton angular frequency $\omega_{\rm DM} \equiv 2\pi f_{\rm DM} = m_{\rm DM}c^2/\hbar$, with a small frequency spread of $\Delta\omega \simeq (v_0^2/c^2)\omega_{\rm DM} \sim 10^{-6}\omega_{\rm DM}$ between volumes. These define coherent regions that travel at an average velocity of v_0, with coherence maintained over the timescale $\tau_{\rm coh} \equiv \lambda_{\rm dB}/v_0 = h/(m_{\rm DM}v_0^2) \approx 21$ h for a DM mass of 10^{-13} eV/c^2. We remain in the coherent regime throughout this work.

Within this regime, the ultralight vector DM field at time t, $\boldsymbol{A}(t)$, traces a three-dimensional ellipse. It can be written as [41,68]

$$\boldsymbol{A}(t) = \frac{\hbar}{m_{\rm DM}c^2}\sqrt{\frac{2\rho_{\rm DM}}{3\varepsilon_0}}\sum_i \alpha_i \cos(\omega_{\rm DM}t + \varphi_i)\hat{\boldsymbol{e}}_i, \quad (1)$$

where ε_0 is the permittivity of free space, and the sum runs over the three components of the field, $i \in \{x, y, z\}$. The parameters α_i and φ_i respectively control the amplitudes and phases of each of the field's components, and they are stochastic. Incorporating the randomness in these variables is crucial for accurate inferences, as this can lead to significant correction factors [53,74–76].

The ultralight vector dark matter field generates new electric and magnetic fields that can couple to ordinary matter. In the case of $B-L$ dark matter, they arise due to a new interaction term in the standard model Lagrangian, $\mathcal{L} \supset -g_{B-L}j^{\mu}_{B-L}A_{\mu}$, where g_{B-L} is the gauge coupling strength, j^{μ}_{B-L} in the new interaction four current, and A^{μ} is the dark matter four field [68]. For nonrelativistic ULDM, the electric field dominates and results in a new Lorentz force, $\boldsymbol{F}(t)$.

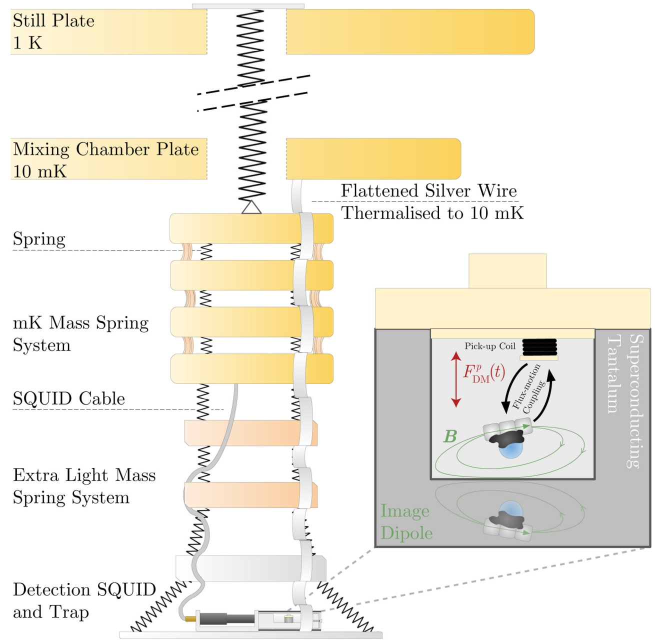

FIG. 1. Schematic of the experimental setup inside the dilution refrigerator. Shown are the plates of the cryostat, the multistage mass-spring system used to shield against external vibrations, and the holder for the trap and magnet. The inset shows the superconducting trap containing the magnet. The effect of the $\boldsymbol{B}$ field can be modeled by an image dipole. The oscillatory force imparted by the ULDM field, $F^p_{\rm DM}(t)$, is also indicated. The black arrows illustrate the coupling of the flux of the moving particle to the pickup coil. Further details and photographs of the setup can be found in Ref. [59].

Our experiment consists of a magnetically levitated particle suspended within a superconducting trap, illustrated in Fig. 1 and described in detail below. We observe the motion of the particle for a time $T_{\rm obs}$, recording it along a single sensitivity axis $\boldsymbol{\zeta}$ via a superconducting pickup coil. This makes the relevant force $F_{\rm DM}(t) \equiv \boldsymbol{\zeta}\cdot\boldsymbol{F}(t)$, where we have approximated $\boldsymbol{\zeta}$ to be static since our observation time is shorter than a day. With the current level of vibration isolation, our experiment is most sensitive along the zenith; we thus align ζ in this direction. Using all three translational degrees of motion would allow us to measure the polarization of the ULDM field in the future.

Accounting for the dynamics of both the trap and the levitated particle, the force experienced by the latter is

$$\begin{aligned} F^p_{\rm DM}(t) \simeq \mathcal{F}[&\alpha_x \cos\lambda\cos\phi\cos(\omega_{\rm DM}t + \varphi_x) \\ &+ \alpha_y \cos\lambda\sin\phi\cos(\omega_{\rm DM}t + \varphi_y) \\ &+ \alpha_z \sin\lambda\cos(\omega_{\rm DM}t + \varphi_z)], \end{aligned} \quad (2)$$

where we have defined the force scale

$$\mathcal{F} \equiv g_{B-L}\left(\mathcal{R}_p - \frac{\omega_0^2}{\omega_{\rm DM}^2}\mathcal{R}_t\right)m_p a_0, \quad (3)$$

with $\mathcal{R}_p$ and $\mathcal{R}_t$ the averaged neutron-to-atomic-weight ratios of the particle and trap, respectively, ω_0 the resonance angular frequency of the particle, m_p the total mass of the particle, and $a_0 \approx 2.12 \times 10^{11}$ ms^{-2} a characteristic acceleration imparted by the ULDM field [68].

We perform inferences in Fourier space by analyzing the force power spectral density (PSD). The PSD will contain the power delivered to our setup by external sources, as well as that supplied by a ULDM signal. When observing for less than a day, the signal is a monochromatic peak in the PSD within the bin containing the Compton frequency. The quantity of interest for our inferencing is the *excess power* at that frequency, defined as the value of the PSD normalized by the expected noise, S_{FF}, within that bin. The excess power is proportional to the square of the dimensionless parameter [68]

$$\kappa \equiv \sqrt{\frac{\mathcal{F}^2 T_{\mathrm{obs}}}{2S_{FF}}}. \tag{4}$$

By measuring the force PSD and fitting to our expected noise level, we perform inferences on κ and map these values to those for the coupling strength, g_{B-L}:

$$g_{B-L} = \frac{\kappa}{|\mathcal{R}_p - (\omega_0^2/\omega_{\mathrm{DM}}^2)\mathcal{R}_t| m_p a_0} \sqrt{\frac{2S_{FF}}{T_{\mathrm{obs}}}}. \tag{5}$$

From this it is clear that magnetic levitation, which affords us the use of heavier particle masses, is an ideal levitation strategy for a bosonic ULDM search.

Experiment—Originally designed to detect small-scale gravity [59], our setup has the force sensitivity and frequency range required of a promising ULDM detector. It features a Type-I superconducting trap with a magnetically levitated permanent magnet composed of three 0.25 mm $Nd_2Fe_{14}B$ cubes and a spherical glass bead of radius 0.25 mm to break rotational symmetry (Fig. 1). The levitated particle has a mass of $m_p \approx 0.43$ mg, a resonance frequency of $f_0 \approx 26.7$ Hz for motions along the zenith, and a quality factor of $Q \approx 9.3 \times 10^6$ [59]. We calculate $\mathcal{R}_p \approx 0.518$ [68].

We detect the motion of the particle using a superconducting pickup loop. The motion of the magnet induces a change in flux in the loop, causing a superconducting current to run in the circuit. This circuit consists of the pickup loop, the calibration loop, and the SQUID input coil, which is inductively coupled to a two-stage direct current SQUID. The calibration loop calibrates the energy coupling between the detection circuit and the degrees of motion of the magnet. We find $\mathcal{R}_t \approx 0.526$ [68].

We shield the trap from environmental vibrations both vertically and laterally using a multistage mass-spring system, and we thermalize the experiment via a flexible silver wire. The closest part of this system, consisting of seven masses, hangs from the still plate, which is suspended from the 3K plate of the cryostat. The cryostat rests on a 25-ton concrete block with pneumatic dampers to reduce vibrations caused by the building. The pulse tube cooler and vacuum pumps are mounted separately.

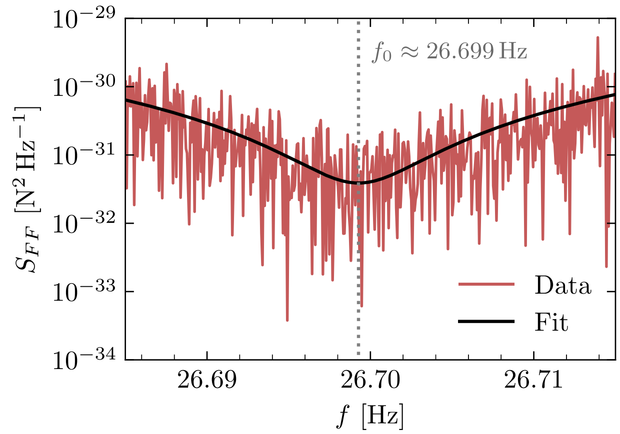

FIG. 2. The force-power spectral density, S_{FF}, with frequency f measured by our experiment. The fit to the force noise background via Eq. (6) is shown. The vertical line highlights the resonance frequency $f_0 \approx 26.699$ Hz relevant for motions parallel to the zenith. Data initially reported in Ref. [59].

The force noise data gathered in Ref. [59] is shown in Fig. 2. The data was continuously recorded on May 13, 2022, over a time of $T_{\mathrm{obs}} \approx 4.2$ h between 22:32 and 02:44 UTC and spans the frequency range 26.6850 Hz–26.7150 Hz. Compared to the original data, we have removed two points: one at the frequency of a generated monochromatic signal (a spinning wheel used for a gravity test) and another at the resonance frequency. The latter was done as the ringdown time of the resonator exceeded the dataset length, so this point represented the starting amplitude of the resonator (see supplement E of Ref. [59]). We fit the data to the total expected force noise via

$$S_{FF}(\omega) = S_{FF}^0 + |\chi(\omega)|^{-2} S_{xx}, \tag{6}$$

where S_{FF}^0 is the force noise arising from the position measurement of the particle, and S_{xx} is the displacement noise due to measurement-added noise from the SQUID. The factor $\chi(\omega) \equiv [m_p(\omega_0^2 - \omega^2 + i\gamma\omega)]^{-1}$ is the mechanical susceptibility, with $\omega_0 \equiv 2\pi f_0$ and $\gamma \equiv \omega_0/Q$. We find the fit values $S_{FF}^0 \approx 3.88 \times 10^{-32}$ N^2 Hz^{-1} and $S_{xx} \approx 3.59 \times 10^{-21}$ m^2 Hz^{-1}.

Data analysis and results—The ULDM signal manifests as a monochromatic peak in the force PSD within the bin containing the Compton frequency, f_{DM}. Its location is dictated by the DM mass, and its noise-normalized amplitude is determined by the parameter κ. We scan over our frequency bins, equivalent to scanning over dark matter masses m_{DM}, and use our measured force PSD to make inferences on the coupling strength, g_{B-L}.

To perform our search, we follow a frequentist approach similar to Ref. [41]. The likelihood of measuring a value for the excess power in any frequency bin is a noncentral χ^2 with two degrees of freedom and a noncentrality parameter controlled by κ. To account for the stochasticity of the ULDM field, we marginalize this likelihood over the three random Rayleigh amplitudes and uniform phases. The result is an exponential likelihood with inverse scale $2+\kappa^2$ [68].

We use this likelihood to define a two-sided test statistic (TS) based on the log-likelihood ratio to ascertain whether a DM signal is present. As our discovery criterion, we require that the excess power yields at least a 3σ significance over the expected background, equivalent to a p value of 2.7×10^{-3}. We evaluate this by first building the distribution of the TS under the null hypothesis that no such signal exists using toy Monte Carlo (MC) simulations. At every frequency bin, we then compute the p value of the data. Our most significant local p value is $p\approx 2.0\times10^{-2}$, which does not exceed our discovery threshold. We therefore turn to setting a limit.

We place 90% confidence level (CL) limits on g_{B-L} using a similar procedure, but taking the signal hypothesis as our null hypothesis. To assess whether our limit is consistent with the background model, we derive the expected median limit and $1\sigma/2\sigma$ limit bands from our setup by simulating background-only pseudodata. We find $\kappa_{\rm lim}^{\rm med}\approx 3.85$, with 1σ and 2σ bands given by $\kappa_{\rm lim}^{1\sigma}\in[2.01,6.47]$ and $\kappa_{\rm lim}^{2\sigma}\in[1.23,9.39]$. Further details on our statistical procedure can be found in Ref. [68].

We show our 90% CL limit in Fig. 3. We find excellent agreement between the results from our MC analysis and our derived limit, which closely follows the median limit and lies well within the 2σ band. Our best constraint is $g_{B-L}\lesssim 2.98\times10^{-21}$, occurring at the DM mass $m_{\rm DM}\approx 1.1042\times10^{-13}$ eV$/c^2$ (Compton frequency $f_{\rm DM}\approx$ 26.6995 Hz). This limit is not as stringent as those set by the fifth-force Eöt-Wash [42,43] and MICROSCOPE [40,41] experiments, falling at $g_{B-L}\lesssim10^{-23}$ and $g_{B-L}\lesssim 2\times10^{-25}$, respectively.

Our limit is the first data-driven constraint on ultralight dark matter using a magnetically levitated particle. However, we derived it using a setup designed for tests of gravity—an orthogonal research objective [59]. We offer a set of experimentally driven upgrades that will make this detector technology a leading option in the search for dark matter, proposing the POLONAISE experiment.

Future prospects—We propose the first optimization of a magnetically levitated setup to achieve leading ULDM sensitivities with POLONAISE. Our key improvement is adding a second coil to control the resonant frequency, allowing us to probe a wider DM mass window. To maximize sensitivity, we aim to reduce force noise, use heavier levitated masses, and increase the neutron-to-atomic-weight ratio difference between the particle and trap.

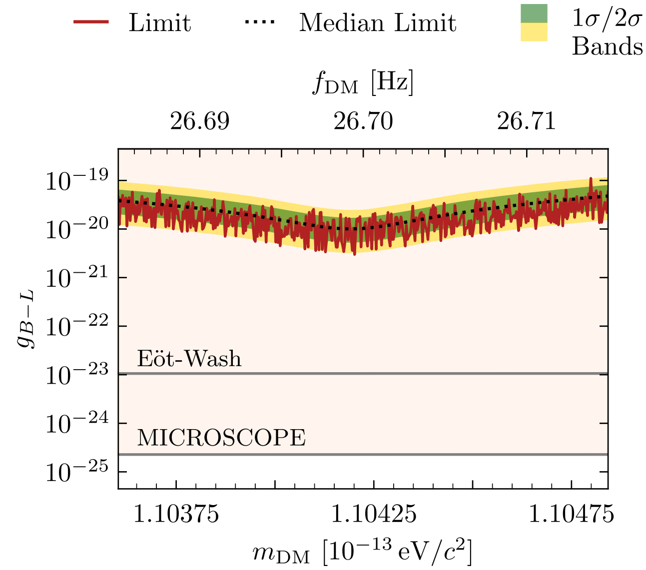

FIG. 3. The 90% confidence level limits on the gauge coupling strength g_{B-L} with dark matter mass $m_{\rm DM}$ (bottom axis) and Compton frequency $f_{\rm DM}$ (top axis). Shown is the data-driven limit derived from the measurements presented in Fig. 2, as well as the median limit and $1\sigma/2\sigma$ bands derived from our Monte Carlo analysis [68]. Also shown are the existing limits from the Eöt-Wash [42,43] and MICROSCOPE [40,41] experiments.

We plan to perform a two-year-long resonant scan with short-, medium-, and long-term upgrades as summarized in Table I. We estimate these upgrades will take three, five, and ten years, respectively. Details on our choices and their impact on our sensitivity can be found in Ref. [68].

At each resonance frequency, f_0, we will measure for 4.05×10^5 Compton cycles to ensure coherence, giving

TABLE I. The short-, medium-, and long-term upgrades for POLONAISE. Shown are the cooling temperature (T), the mass of the levitated particle (m_p), the SQUID energy resolution ($n_{\rm SQ}$), the total root force PSD ($\sqrt{S_{FF}}$), the bandwidth that optimizes the expected force noise ($\Delta f_{\rm opt}$), the quality factor (Q), the difference between the neutron-to-atomic-weight ratios of the levitated particle and trap ($|\mathcal{R}_p-\mathcal{R}_t|$), and the number of levitated particles employed (N_p). At each resonance frequency, f_0, the measurement time is $T_{\rm obs}=4.05\times10^5/f_0$.

	Short	Medium	Long
T [mK]	20	20	2
m_p [mg]	0.43	430	430
$n_{\rm SQ}$ [$\hbar$]	10^3	10^2	10^1
$\sqrt{S_{FF}}$ [N/$\sqrt{\rm Hz}$]	$10^{-19}f_0^{1/2}$	$10^{-18}f_0^{1/2}$	$10^{-19}f_0^{1/2}$
$\Delta f_{\rm opt}$ [mHz]	3.4	3.4	0.34
Q	10^8	10^9	10^{10}
$\lvert\mathcal{R}_p-\mathcal{R}_t\rvert$	0.039	0.039	0.213
N_p	1	10	100

$T_{\mathrm{obs}} = 4.05 \times 10^5/f_0$. We will match our frequency steps to the optimal bandwidth, Δf_{opt}, that maximizes our sensitivity while minimizing noise by tuning the SQUID coupling to have equal backaction and thermal noise. Cooling will reach 20 mK (short and medium terms) and 2 mK (long-term) using nuclear demagnetization [77]. We will improve the quality factor by using insulating magnets to reduce Eddy current damping [78] and improve SQUID energy resolution with alternating current readouts [79]. Avoiding interference in the SQUID readout will reduce n_{SQ} by factors of 10 (short-term) and 100–1,000 (medium/long term) with radio frequency readouts [58]. We will parallelize our scan by using multiple levitated particles monitored by a single SQUID, which can read out multiple pickup coils in series by designing the traps to have nonoverlapping resonance frequencies. The number of SQUIDS is scalable, with a commercial dilution refrigerator able to house up to 100 SQUIDs. In the short term, we will scan a range of 21 Hz–35 Hz, extending this to 10 Hz–200 Hz in the medium and long terms. This scan is realizable by adding a coil inside the superconducting trap and using a DC current to tune the resonance frequencies. Using a persistent current will minimize current-added noise [80].

Exploiting magnetic levitation's ability to support heavier objects, we will improve our sensitivity by increasing the particle mass to 43 mg (short term) and 430 mg (medium/long term). Maintaining force noise and reducing trap vibrations will be challenging as the spring constant increases with mass, requiring vibration isolation improvements of 40 dB, 80 dB, and 100 dB at 25 Hz for each of our upgrades, respectively. This is feasible since the required isolation is comparable to LIGO's performance but only needed around the particle's resonance frequency [81]. Finally, by optimizing the experiment materials, we will improve $|\mathcal{R}_p - \mathcal{R}_t|$ to 0.039 (short/medium term) and 0.213 (long term) [68]. For our long-term goal, we will attach a thin-walled aluminium container filled with one liter of solid hydrogen.

We show the projected 90% CL limits on the coupling strength from our proposed upgrades in Fig. 4. To compute them, we have used our derived value of $\kappa_{\mathrm{lim}}^{\mathrm{med}} \approx 3.85$ in Eq. (5), giving us projections assuming a background-only measurement. Our short-term upgrade is competitive with Eöt-Wash [42,43], and our medium- and long-term configurations probe new areas of parameter space. Our medium-term limit surpasses that of Eöt-Wash for all scanned masses, is competitive with MICROSCOPE at low masses, and constrains new couplings beyond those of MICROSCOPE and LIGO/Virgo [43,44] at high masses. Our long-term limit is leading, going beyond the limit set by MICROSCOPE [40,41] by 2 orders of magnitude at lower masses and that set by LIGO/Virgo by 3 orders of magnitude at higher masses.

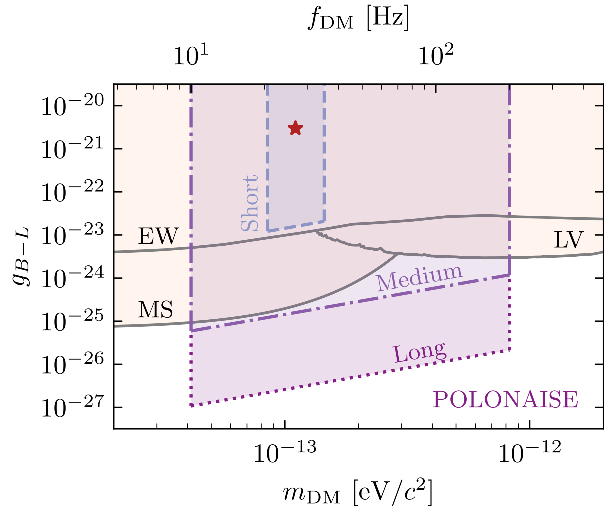

FIG. 4. Projected 90% confidence level limits on the gauge coupling strength g_{B-L} with dark matter mass m_{DM} (bottom axis) and Compton frequency f_{DM} (top axis) for POLONAISE. Projections are based on the short-, medium-, and long-term configurations detailed in Table I. Also shown is our current best limit from Fig. 3 (red star), as well as the existing limits from the MICROSCOPE (MS) [40,41], Eöt-Wash (EW) [42,43], and LIGO/Virgo (LV) [43,44] experiments.

Conclusions—We have performed the first search for ultralight dark matter using a magnetically levitated particle. Focusing on dark matter coupled to the difference between baryon and lepton number, $B - L$, we have found no significant evidence of a signal in the mass range $(1.10360 - 1.10485) \times 10^{-13}$ eV/c^2, equivalent to the frequency range 26.6850 Hz–26.7150 Hz. We have set a 90% confidence level limit on the coupling strength, finding the best constraint to be $g_{B-L} \lesssim 2.98 \times 10^{-21}$. We have proposed the POLONAISE experiment, featuring short-, medium-, and long-term improvements to our setup to enable sensitivity to unexplored model parameter space. Our result highlights the promise of this quantum sensing technology in the hunt for dark matter, and we hope that it fuels initiatives in advancing experimental designs of magnetically levitated setups for astroparticle physics.

Acknowledgments—We would like to thank Daniel Carney, Andrew Long, Bas Hensen, Mudit Jain, Martijn Janse, and Yue Zhao for their valuable feedback on the manuscript. D. A. would like to thank Juehang Qin for helpful discussions throughout this work, especially concerning our statistical treatment, as well as Mustafa Amin for discussions regarding the ultralight dark matter field. D. A. and C. T. were jointly funded by Rice University and NSF Award No. 2046549. T. O. acknowledges funding from NWO Grant No. OCENW.GROOT.2019.088. D. U. and T. O. were jointly funded by the EU Horizon Europe EIC Pathfinder Project QuCoM (Grant No. 10032223).

[1] G. Bertone and D. Hooper, History of dark matter, Rev. Mod. Phys. **90**, 045002 (2018).
[2] K. Freese, Status of dark matter in the universe, Int. J. Mod. Phys. **1**, 325 (2017).
[3] M. Cirelli, A. Strumia, and J. Zupan, Dark matter, arXiv:2406.01705.
[4] T. D. Brandt, Constraints on MACHO dark matter from compact stellar systems in ultra-faint dwarf galaxies, Astrophys. J. Lett. **824**, L31 (2016).
[5] N. Dalal and A. Kravtsov, Excluding fuzzy dark matter with sizes and stellar kinematics of ultrafaint dwarf galaxies, Phys. Rev. D **106**, 063517 (2022).
[6] R. Essig *et al.*, Working Group Report: New light weakly coupled particles, in *Proceedings of the Snowmass 2013: Snowmass on the Mississippi* (2013), arXiv:1311.0029.
[7] D. Antypas *et al.*, New horizons: Scalar and vector ultralight dark matter, arXiv:2203.14915.
[8] S. Weinberg, A new light boson?, Phys. Rev. Lett. **40**, 223 (1978).
[9] F. Wilczek, Problem of strong P and T invariance in the presence of instantons, Phys. Rev. Lett. **40**, 279 (1978).
[10] L. Di Luzio, M. Giannotti, E. Nardi, and L. Visinelli, The landscape of QCD axion models, Phys. Rep. **870**, 1 (2020).
[11] A. Arvanitaki, S. Dimopoulos, S. Dubovsky, N. Kaloper, and J. March-Russell, String axiverse, Phys. Rev. D **81**, 123530 (2010).
[12] A. Ringwald, Axions and axion-like particles, in *Proceedings of the 49th Rencontres de Moriond on Electroweak Interactions and Unified Theories* (2014), pp. 223–230, arXiv:1407.0546.
[13] E. G. M. Ferreira, Ultra-light dark matter, Astron. Astrophys. Rev. **29**, 7 (2021).
[14] J. Jaeckel, A force beyond the Standard Model—Status of the quest for hidden photons, Frascati Phys. Ser. **56**, 172 (2012), https://inspirehep.net/literature/1223126.
[15] M. Fabbrichesi, E. Gabrielli, and G. Lanfranchi, *The Physics of the Dark Photon: A Primer*, SpringerBriefs in Physics (Springer, Cham, 2020), 10.1007/978-3-030-62519-1.
[16] A. Caputo, A. J. Millar, C. A. J. O'Hare, and E. Vitagliano, Dark photon limits: A handbook, Phys. Rev. D **104**, 095029 (2021).
[17] P. W. Graham, J. Mardon, and S. Rajendran, Vector dark matter from inflationary fluctuations, Phys. Rev. D **93**, 103520 (2016).
[18] P. Agrawal, N. Kitajima, M. Reece, T. Sekiguchi, and F. Takahashi, Relic abundance of dark photon dark matter, Phys. Lett. B **801**, 135136 (2020).
[19] R. T. Co, A. Pierce, Z. Zhang, and Y. Zhao, Dark photon dark matter produced by axion oscillations, Phys. Rev. D **99**, 075002 (2019).
[20] J. A. Dror, K. Harigaya, and V. Narayan, Parametric resonance production of ultralight vector dark matter, Phys. Rev. D **99**, 035036 (2019).
[21] M. Bastero-Gil, J. Santiago, L. Ubaldi, and R. Vega-Morales, Vector dark matter production at the end of inflation, J. Cosmol. Astropart. Phys. 04 (2019) 015.
[22] A. J. Long and L.-T. Wang, Dark photon dark matter from a network of cosmic strings, Phys. Rev. D **99**, 063529 (2019).
[23] E. W. Kolb and A. J. Long, Completely dark photons from gravitational particle production during the inflationary era, J. High Energy Phys. 03 (2021) 283.
[24] R. T. Co, K. Harigaya, and A. Pierce, Gravitational waves and dark photon dark matter from axion rotations, J. High Energy Phys. 12 (2021) 099.
[25] P. Adshead, K. D. Lozanov, and Z. J. Weiner, Dark photon dark matter from an oscillating dilaton, Phys. Rev. D **107**, 083519 (2023).
[26] D. Cyncynates and Z. J. Weiner, Detectable, defect-free dark photon dark matter, arXiv:2310.18397.
[27] O. Özsoy and G. Tasinato, Vector dark matter, inflation, and non-minimal couplings with gravity, J. Cosmol. Astropart. Phys. 06 (2024) 003.
[28] M. A. Amin, M. Jain, R. Karur, and P. Mocz, Small-scale structure in vector dark matter, J. Cosmol. Astropart. Phys. 08 (2022) 014.
[29] M. Gorghetto, E. Hardy, J. March-Russell, N. Song, and S. M. West, Dark photon stars: Formation and role as dark matter substructure, J. Cosmol. Astropart. Phys. 08 (2022) 018.
[30] M. Jain and M. A. Amin, i-SPin: An integrator for multicomponent Schrödinger-Poisson systems with self-interactions, J. Cosmol. Astropart. Phys. 04 (2023) 053.
[31] M. Jain, M. A. Amin, J. Thomas, and W. Wanichwecharungruang, Kinetic relaxation and Bose-star formation in multicomponent dark matter, Phys. Rev. D **108**, 043535 (2023).
[32] M. Jain, M. A. Amin, and H. Pu, Integrator for general spin-s Gross-Pitaevskii systems, Phys. Rev. E **108**, 055305 (2023).
[33] P. Fayet, Effects of the spin 1 partner of the goldstino (gravitino) on neutral current phenomenology, Phys. Lett. **95B**, 285 (1980).
[34] P. Fayet, On the search for a new spin 1 boson, Nucl. Phys. **B187**, 184 (1981).
[35] M. E. Peskin and D. V. Schroeder, *An Introduction to Quantum Field Theory* (Addison-Wesley, Reading, 1995).
[36] L. Basso, A. Belyaev, S. Moretti, and C. H. Shepherd-Themistocleous, Phenomenology of the minimal $B-L$ extension of the standard model: Z' and neutrinos, Phys. Rev. D **80**, 055030 (2009).
[37] S. Kanemura, T. Matsui, and H. Sugiyama, Neutrino mass and dark matter from gauged $U(1)_{B-L}$ breaking, Phys. Rev. D **90**, 013001 (2014).
[38] P. Touboul *et al.*, MICROSCOPE Mission: First results of a space test of the equivalence principle, Phys. Rev. Lett. **119**, 231101 (2017).
[39] J. Bergé, P. Brax, G. Métris, M. Pernot-Borràs, P. Touboul, and J.-P. Uzan, MICROSCOPE mission: First constraints on the violation of the weak equivalence principle by a light scalar dilaton, Phys. Rev. Lett. **120**, 141101 (2018).
[40] P. Touboul *et al.* (MICROSCOPE Collaboration), MICROSCOPE mission: Final results of the test of the equivalence principle, Phys. Rev. Lett. **129**, 121102 (2022).
[41] D. W. P. Amaral, M. Jain, M. A. Amin, and C. Tunnell, Vector wave dark matter and terrestrial quantum sensors, J. Cosmol. Astropart. Phys. 06 (2024) 050.

[42] T. A. Wagner, S. Schlamminger, J. H. Gundlach, and E. G. Adelberger, Torsion-balance tests of the weak equivalence principle, Classical Quantum Gravity **29**, 184002 (2012).

[43] C. O'Hare, cajohare/axionlimits: Axionlimits, (2020), https://cajohare.github.io/AxionLimits/.

[44] R. Abbott *et al.* (LIGO Scientific, KAGRA, and Virgo Collaborations), Constraints on dark photon dark matter using data from LIGO's and Virgo's third observing run, Phys. Rev. D **105**, 063030 (2022).

[45] A. G. Abac *et al.* (LIGO Scientific, VIRGO, and KAGRA Collaborations), Ultralight vector dark matter search using data from the KAGRA O3GK run, Phys. Rev. D **110**, 042001 (2024).

[46] P. W. Graham, D. E. Kaplan, J. Mardon, S. Rajendran, and W. A. Terrano, Dark matter direct detection with accelerometers, Phys. Rev. D **93**, 075029 (2016).

[47] D. Carney *et al.*, Mechanical quantum sensing in the search for dark matter, Quantum Sci. Technol. **6**, 024002 (2021).

[48] D. Carney, A. Hook, Z. Liu, J. M. Taylor, and Y. Zhao, Ultralight dark matter detection with mechanical quantum sensors, New J. Phys. **23**, 023041 (2021).

[49] J. Manley, M. D. Chowdhury, D. Grin, S. Singh, and D. J. Wilson, Searching for vector dark matter with an optomechanical accelerometer, Phys. Rev. Lett. **126**, 061301 (2021).

[50] M. Abe, P. Adamson, M. Borcean, D. Bortoletto, K. Bridges, S. P. Carman, S. Chattopadhyay, J. Coleman, N. M. Curfman, K. DeRose *et al.*, Matter-wave atomic gradiometer interferometric sensor (MAGIS-100), Quantum Sci. Technol. **6**, 044003 (2021).

[51] A. Pierce, K. Riles, and Y. Zhao, Searching for dark photon dark matter with gravitational wave detectors, Phys. Rev. Lett. **121**, 061102 (2018).

[52] S. Morisaki, T. Fujita, Y. Michimura, H. Nakatsuka, and I. Obata, Improved sensitivity of interferometric gravitational wave detectors to ultralight vector dark matter from the finite light-traveling time, Phys. Rev. D **103**, L051702 (2021).

[53] H. Nakatsuka, S. Morisaki, T. Fujita, J. Kume, Y. Michimura, K. Nagano, and I. Obata, Stochastic effects on observation of ultralight bosonic dark matter, Phys. Rev. D **108**, 092010 (2023).

[54] M. A. Fedderke and A. Mathur, Asteroids for ultralight dark-photon dark-matter detection, Phys. Rev. D **107**, 043004 (2023).

[55] A. Vinante, P. Falferi, G. Gasbarri, A. Setter, C. Timberlake, and H. Ulbricht, Ultralow mechanical damping with Meissner-levitated ferromagnetic microparticles, Phys. Rev. Appl. **13**, 064027 (2020).

[56] J. Hofer, R. Gross, G. Higgins, H. Huebl, O. F. Kieler, R. Kleiner, D. Koelle, P. Schmidt, J. A. Slater, M. Trupke, K. Uhl, T. Weimann, W. Wieczorek, and M. Aspelmeyer, High-Q magnetic levitation and control of superconducting microspheres at millikelvin temperatures, Phys. Rev. Lett. **131**, 043603 (2023).

[57] M. G. Latorre, G. Higgins, A. Paradkar, T. Bauch, and W. Wieczorek, Superconducting microsphere magnetically levitated in an anharmonic potential with integrated magnetic readout, Phys. Rev. Appl. **19**, 054047 (2023).

[58] P. Schmidt *et al.*, Remote sensing of a levitated superconductor with a flux-tunable microwave cavity, Phys. Rev. Appl. **22**, 014078 (2024).

[59] T. M. Fuchs, D. G. Uitenbroek, J. Plugge, N. van Halteren, J.-P. van Soest, A. Vinante, H. Ulbricht, and T. H. Oosterkamp, Measuring gravity with milligram levitated masses, Sci. Adv. **10**, eadk2949 (2024).

[60] M. Janse, D. G. Uitenbroek, L. van Everdingen, J. Plugge, B. Hensen, and T. H. Oosterkamp, Current experimental upper bounds on spacetime diffusion, Phys. Rev. Res. **6**, 033076 (2024).

[61] G. Higgins, S. Kalia, and Z. Liu, Maglev for dark matter: Dark-photon and axion dark matter sensing with levitated superconductors, Phys. Rev. D **109**, 055024 (2024).

[62] R. Li, S. Lin, L. Zhang, C. Duan, P. Huang, and J. Du, Search for ultralight dark matter with a frequency adjustable diamagnetic levitated sensor, Chin. Phys. Lett. **40**, 069502 (2023).

[63] S. Kalia, D. Budker, D. F. J. Kimball, W. Ji, Z. Liu, A. O. Sushkov, C. Timberlake, H. Ulbricht, A. Vinante, and T. Wang, Ultralight dark matter detection with levitated ferromagnets, Phys. Rev. D **110**, 115029 (2024).

[64] E. Kilian *et al.*, Dark matter searches with levitated sensors, AVS Quantum Sci. **6**, 030503 (2024).

[65] R. Catena and P. Ullio, A novel determination of the local dark matter density, J. Cosmol. Astropart. Phys. 08 (2010) 004.

[66] J. I. Read, The local dark matter density, J. Phys. G **41**, 063101 (2014).

[67] N. W. Evans, C. A. J. O'Hare, and C. McCabe, Refinement of the standard halo model for dark matter searches in light of the Gaia Sausage, Phys. Rev. D **99**, 023012 (2019).

[68] See Supplemental Material at http://link.aps.org/supplemental/10.1103/PhysRevLett.134.251001, which includes Refs. [69–73], for further details on ultralight vector dark matter theory and signal, employed statistics, and future experiments.

[69] S. Chaudhuri, P. W. Graham, K. Irwin, J. Mardon, S. Rajendran, and Y. Zhao, Radio for hidden-photon dark matter detection, Phys. Rev. D **92**, 075012 (2015).

[70] G. Cowan, K. Cranmer, E. Gross, and O. Vitells, Asymptotic formulae for likelihood-based tests of new physics, Eur. Phys. J. C **71**, 1554 (2011); **73**, 2501(E) (2013).

[71] M. A. Fedderke, P. W. Graham, D. F. J. Kimball, and S. Kalia, Earth as a transducer for dark-photon dark-matter detection, Phys. Rev. D **104**, 075023 (2021).

[72] P. W. Graham, J. Mardon, S. Rajendran, and Y. Zhao, Parametrically enhanced hidden photon search, Phys. Rev. D **90**, 075017 (2014).

[73] E. J. Groth, Probability distributions related to power spectra, Astrophys. J. Suppl. Ser. **29**, 285 (1975).

[74] J. W. Foster, N. L. Rodd, and B. R. Safdi, Revealing the dark matter halo with axion direct detection, Phys. Rev. D **97**, 123006 (2018).

[75] G. P. Centers *et al.*, Stochastic fluctuations of bosonic dark matter, Nat. Commun. **12**, 7321 (2021).

[76] M. Lisanti, M. Moschella, and W. Terrano, Stochastic properties of ultralight scalar field gradients, Phys. Rev. D **104**, 055037 (2021).

[77] B. van Heck, T. M. Fuchs, J. Plugge, W. A. Bosch, and T. H. Oosterkamp, Magnetic cooling and vibration isolation of a sub-kHz mechanical resonator, J. Low Temp. Phys. **210**, 588 (2023).

[78] C. Timberlake, G. Gasbarri, A. Vinante, A. Setter, and H. Ulbricht, Acceleration sensing with magnetically levitated oscillators above a superconductor, Appl. Phys. Lett. **115**, 224101 (2019).

[79] M. Mück, J. Kycia, and J. Clarke, Superconducting quantum interference device as a near-quantum-limited amplifier at 0.5 GHz, Appl. Phys. Lett. **78**, 967 (2001).

[80] B. van Waarde, O. Benningshof, and T. Oosterkamp, A magnetic persistent current switch at milliKelvin temperatures, Cryogenics **78**, 74 (2016).

[81] M. Maggiore *et al.*, Science case for the Einstein telescope, J. Cosmol. Astropart. Phys. 03 (2020) 050.